JNS

LABORATORY INVESTIGATION

J Neurosurg 137:1431–1442, 2022

Microsurgical anatomy and the importance of the petrosal process of the sphenoid bone in endonasal surgery

Ayoze Doniz-Gonzalez, MD,[1,2] Vera Vigo, MD,[1] Maximiliano Alberto Nunez, MD,[1,3] Yuanzhi Xu, MD,[1,4] Ahmed Mohyeldin, MD, PhD,[1] Aaron A. Cohen-Gadol, MD, MSc, MBA,[5,6] and Juan C. Fernandez-Miranda, MD[1,6]

[1]Department of Neurosurgery, Stanford Hospital, Stanford, California; [2]Department of Neurosurgery, Hospital Universitario de Canarias, La Laguna, Spain; [3]Department of Neurosurgery, Hospital El Cruce, Buenos Aires, Argentina; [4]Department of Neurosurgery, Huashan Hospital, Shanghai Medical College, Fudan University, Shanghai, China; [5]Department of Neurological Surgery, Indiana University, Indianapolis; and [6]*The Neurosurgical Atlas*, Carmel, Indiana

OBJECTIVE The petrosal process of the sphenoid bone (PPsb) is a relevant skull base osseous prominence present bilaterally that can be used as a key surgical landmark, especially for identifying the abducens nerve. The authors investigated the surgical anatomy of the PPsb, its relationship with adjacent neurovascular structures, and its practical application in endoscopic endonasal surgery.

METHODS Twenty-one dried skulls were used to analyze the osseous anatomy of the PPsb. A total of 16 fixed silicone-injected postmortem heads were used to expose the PPsb through both endonasal and transcranial approaches. Dimensions and distances of the PPsb from the foramen lacerum (inferiorly) and top of the posterior clinoid process (PCP; superiorly) were measured. Moreover, anatomical variations and the relationship of the PPsb with the surrounding crucial structures were recorded. Three representative cases were selected to illustrate the clinical applications of the findings.

RESULTS The PPsb presented as a triangular bony prominence, with its base medially adjacent to the dorsum sellae and its apex pointing posterolaterally toward the petrous apex. The mean width of the PPsb was 3.5 ± 1 mm, and the mean distances from the PPsb to the foramen lacerum and the PCP were 5 ± 1 and 11 ± 2.5 mm, respectively. The PPsb is anterior to the petroclival venous confluence, superomedial to the inferior petrosal sinus, and inferomedial to the superior petrosal sinus; constitutes the inferomedial limit of the cavernous sinus; and delimits the upper limit of the paraclival internal carotid artery (ICA) before the artery enters the cavernous sinus. The PPsb is anterior and medial to and below the sixth cranial nerve, forming the floor of Dorello's canal. During surgery, gentle mobilization of the paraclival ICA reveals the petrosal process, serving as an accurate landmark for the location of the abducens nerve.

CONCLUSIONS This investigation revealed details of the microsurgical anatomy of the PPsb, its anatomical relationships, and its application as a surgical landmark for identifying the abducens nerve. This novel landmark may help in minimizing the risk of abducens nerve injury during transclival approaches, which extend laterally toward the petrous apex and cavernous sinus region.

https://thejns.org/doi/abs/10.3171/2021.12.JNS212024

KEYWORDS endoscopic endonasal approach; petrosal process of the sphenoid bone; abducens nerve; internal carotid artery; cavernous sinus; petroclival dural fold; pituitary surgery

Advancements in the field of endoscopic endonasal surgery have led to extended approaches to skull base tumors.[1–3] To achieve optimal tumor resection and avoid neurovascular injury,[4] knowledge of the surgical neuroanatomy and key landmarks for identifying relevant structures is essential.[5] When approaching a lesion that extends laterally into the petroclival and cavernous sinus (CS) regions, the abducens nerve (cranial nerve [CN] VI) is at significant risk given its medial location and trajectory compared to those of other CNs.[6] Several landmarks have been proposed for identifying CN VI;[7–10] however, none of them have been proven to be consistently reliable and accurate.

The petrous or petrosal process of the sphenoid bone

ABBREVIATIONS CN = cranial nerve; CS = cavernous sinus; DMA = dorsal meningeal artery; EEAtt = endoscopic endonasal transclival transpterygoid approach; FL = foramen lacerum; ICA = internal carotid artery; IPS = inferior petrosal sinus; LPsb = lingual process of the sphenoid bone; PCDF = petroclival dural fold; PCF = petroclival fissure; PCP = posterior clinoid process; PLL = petrolingual ligament; PPsb = petrosal process of the sphenoid bone; PVC = petroclival venous confluence; SPS = superior petrosal sinus.

SUBMITTED August 23, 2021. **ACCEPTED** December 16, 2021.
INCLUDE WHEN CITING Published online March 11, 2022; DOI: 10.3171/2021.12.JNS212024.

(PPsb) was first described by Henry Gray in the early 20th century as a "sharp process below the notch for the passage of the abducens nerve on either side of the dorsum sellae of the sphenoid bone."[11] The PPsb is present bilaterally, and each can be outlined as a triangular bony prominence on the side of the dorsum sellae, which articulates laterally with the apex of the petrous portion of the temporal bone. The PPsb continues medially and inferiorly with the clivus and superiorly with the posterior clinoid process (PCP).

In this anatomical study, we investigated the anatomy of the PPsb and its relationship with the surrounding osseus, dural, and neurovascular structures. We propose the PPsb as a key surgical landmark for CN VI and demonstrate its surgical application with 3 illustrative cases.

Methods

Osteological Study

Twenty-one dried human skulls were used for studying the osseous anatomy of the upper petroclival junction and the PPsb. The distances between the PPsb and the PCP, foramen lacerum (FL), and sellar floor were measured bilaterally and recorded with a digital micrometer, as were the widths of the PPsb and dorsum sellae, and the distance between both petrous apices. All data were analyzed with SPSS version 26.0 (IBM Corp.), and values are shown as the mean ± standard deviation. A volumetric model of one of the skulls was created using photogrammetry to better emphasize the osseus relationships of the PPsb with other structures.[12–14]

Anatomical Study

Sixteen lightly embalmed latex-injected postmortem heads were used in this study. An endoscopic endonasal transclival transpterygoid approach (EEAtt) was used in 10 heads.[15] The dissections were performed using lens endoscopes (0°, 30°, and 45°; Karl Storz SE & Co. KG). The heads were positioned supine, slightly rotated toward the surgeon, and fixed with a head holder (Mayfield Stabilization, Integra LifeSciences Corporation) to simulate a surgical position. A neuronavigation system (StealthStation, Medtronic) was used to record measurements and identify the PPsb and petroclival fissure (PCF). The distance between the PPsb with the pterygosphenoidal fissure and the sellar floor was measured, as was the angle formed by the paraclival internal carotid artery (ICA) and PCF. The anatomical relationships of the PPsb with dural, venous, arterial, and neural structures were described and the variations recorded.

Anatomical dissections from the transcranial perspective were performed in 6 additional specimens that were used to compare the endonasal and microsurgical views of the PPsb. In 4 of these heads, to identify the structures at the skull base the cranial convexity and brain were removed, leaving the dura and the nerves attached. In addition, in 1 of the remaining 2 head specimens, an extended middle fossa approach[16] was performed to expose the interdural and cavernous segments of CN VI. The lateral wall of the CS was dissected, and the lateral aspect of the PPsb was exposed through the infratrochlear triangle with the aid of a surgical microscope (HS Hi-R 1000G, Haag-Streit). The distance between CN VI and the posterior petroclinoidal dural fold was measured by using a surgical ruler before and after drilling the PPsb and releasing and transposing CN VI inferiorly. In the remaining specimen, a combined transpetrosal approach[17,18] was performed to identify the cisternal, interdural, and cavernous segments of CN VI and to get a posterolateral view of the PPsb. The distance from the medial edge of the paraclival ICA to the PCF was measured bilaterally.

Three additional lightly embalmed latex-injected postmortem head specimens were selected to reconstruct a volumetric model of the endoscopic endonasal and transcranial views of the PPsb by using the photogrammetry technique.[12–14]

Institutional review board/ethics committee approval and patient consent were neither required nor sought for this study.

TABLE 1. Descriptive statistics: results of the osteological study

	No. of Specimens	Measurements, mm			
		Mean	SD	Min	Max
PPsb width					
Rt	21	3.52	1.13	2	6
Lt	21	3.35	1.26	2	6
DS width	21	15.64	2.11	11	20
Distance					
PA to PA	21	22.38	2.13	18	26
PPsb to PCP					
Rt	20	11.05	2.18	8	16
Lt	20	10.55	2.39	7	17
Sella to PCP					
Rt	20	6.15	2.23	2	10
Lt	20	5.6	2.47	2	10
PPsb to FL					
Rt	21	5.02	1.40	3	9
Lt	21	4.85	0.79	3	6
FL to PCP					
Rt	20	15.2	2.44	11	20
Lt	20	15.1	2.65	11	19

DS = dorsum sellae; PA = petrous apex.

Results

The PPsb was identified bilaterally in each dried skull examined, and the measurements recorded are shown in Table 1. In 2 skulls, 1 of the PCPs was missing, so for each of these 2 skulls, the mean of the total was taken to estimate the measures in which it was involved.

In every human head in our study, we investigated the anatomical relationships of the different structures with the PPsb from endonasal and transcranial perspectives. The findings are categorized here as osseous, dural, venous, arterial, and neural relationships. A technical nuance regarding the surgical identification of the PPsb is also described below.

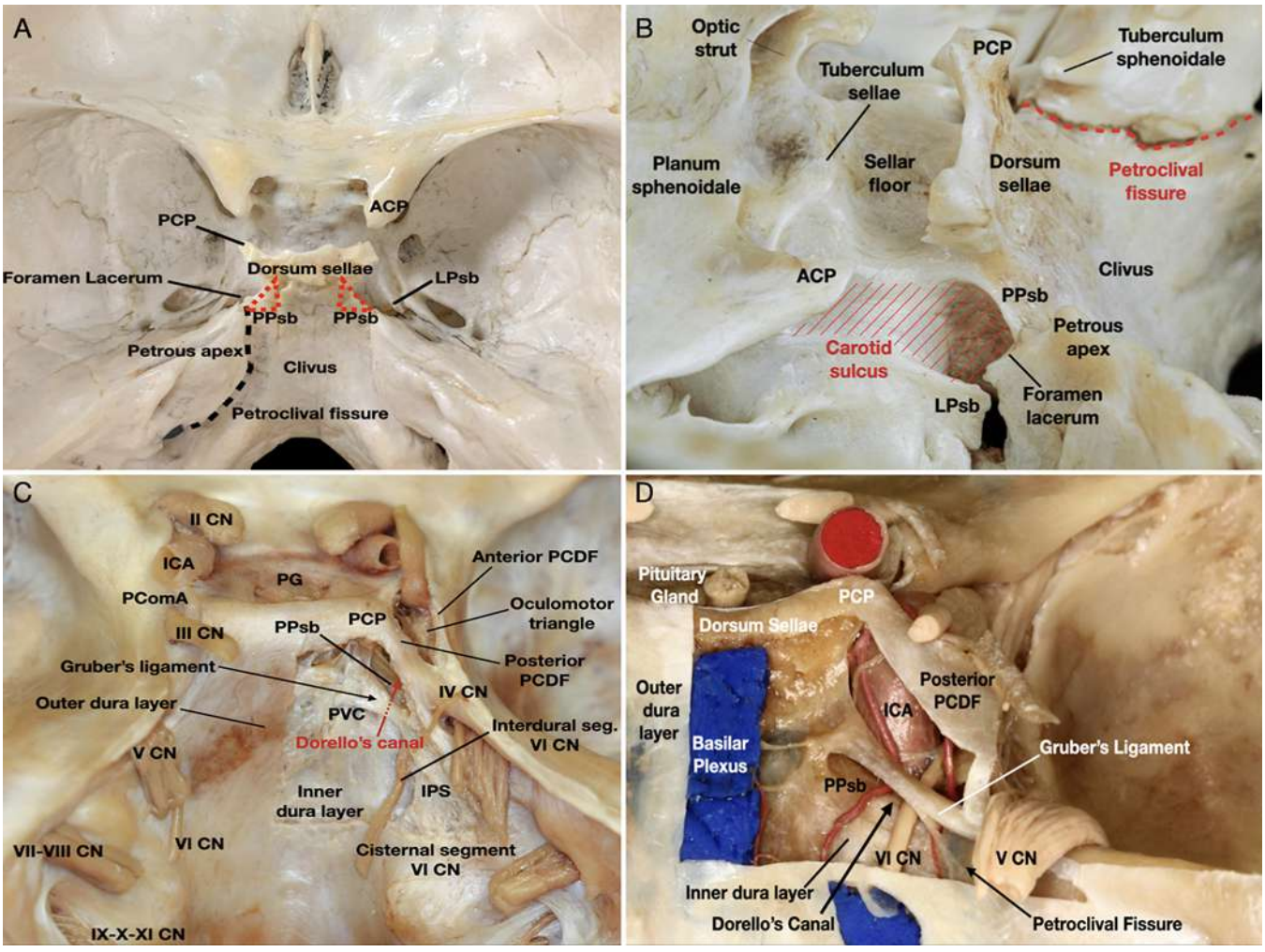

FIG. 1. Osseus and dural relationships of the petrosal process of the sphenoid bone (PPsb). **A:** Posterosuperior view. The clivus lies between the foramen posteroinferiorly and the dorsum sellae anterosuperiorly. The PPsb (*red dotted triangles*) is medial to the PCF (*black dotted line*), while the petrous apex is lateral to it. **B:** Lateral view. The PPsb and lingual process of the sphenoid bone (LPsb) constitute the medial and lateral borders of the carotid sulcus (*red lines*) and FL. The petrous apex is lateral to the PCF (*red dotted line*). The inferior attachment of Gruber's ligament is at the tuberculum sphenoidale of the petrous apex. **C:** Overview of dural relationships. The brain has been removed, preserving the cranial nerves (CNs). The meningeal layer is the first that CN VI pierces in an inferior to superior, medial to lateral trajectory. The cisternal segment of CN VI can be identified. The inner dural layer has been opened in the right side, leaving the outer dural layer attached. The interdural segment of CN VI can be identified running inside the petroclival venous confluence (PVC). Gruber's ligament runs from the dorsum sellae to the petrous apex, forming the roof of Dorello's canal. **D:** CN VI runs below Gruber's ligament and bends above the PPsb, entering the CS. ACP = anterior clinoid process; ICA = internal carotid artery; IPS = inferior petrosal sinus; PCDF = petroclival dural fold; PComA = posterior communicating artery; PCP = posterior clinoid process; PG = pituitary gland. With permission from Juan C. Fernandez-Miranda and *The Neurosurgical Atlas* by Aaron A. Cohen-Gadol. Figure is available in color online only.

Osseous Relationships

The PPsb is located at both sides of the dorsum sellae, and its lower margin continues with the spheno-occipital synchondrosis[5] (see model 1, https://sketchfab.com/3d-models/skull-base-ef3f369b2938461ab2f2492afa0729be, a 3D volumetric skull base model showing the PPsb and its relationship with the relevant osseus structures). PPsb morphology resembles a triangle or wedge, with its base located medially and its apex pointing posterolaterally to the petrous apex (Fig. 1A).

The PPsb continues posterolaterally with the petrous apex and inferomedially with the FL. The PPsb has a variable length and slope from its superomedial portion to its lateral and more inferior end. In some cases, the PPsb can be narrow, with a sharp transition between the clival portion of the sphenoid bone and the petrous apex. The PPsb is medial to the PCF (Fig. 1B).

From an anterior view, the PPsb constitutes the lateral extension of the clivus behind both paraclival ICAs. The PPsb is not at the same axial plane as the floor of the sella turcica, being a mean of 3.5 ± 0.5 mm inferior to it. From the FL, the PPsb apex is a mean of 5 ± 1 mm superior to the floor of the sella turcica. The petrous apex is indeed lateral to the PCF and hidden behind the ICA in an antero-

posterior view. The mean distance from the medial edge of the ICA to the PCF was 4 ± 1 mm.

Regarding the pneumatization of the sphenoid sinus,[19] the PPsb can be visualized differently. In a sellar type, the PPsb forms a recess between the paraclival ICA and the clival recess itself, which we describe as the carotidoclival recess. In a presellar or conchal type, the PPsb constitutes a bony wedge posterior to the paraclival ICA, as described above.

Dural Relationships

The clival surface is covered by 2 dural layers, the inner and outer layers[20] (Fig. 1C), with the basilar plexus running between them. The meningeal (inner) layer is pierced by CN VI as it transitions from the cisternal to the interdural segment.[6,7,21,22] Between the periosteal and meningeal dural layers are several connective bands, including Gruber's or the petrosphenoidal ligament (Fig. 1D). This ligament is the thickest and most constant, running from the posterior surface of the petrous apex to the dorsum sellae,[23] forming the roof of Dorello's canal. CN VI was found underneath Gruber's ligament in each of our specimens (see model 2, https://sketchfab.com/3d-models/skull-base-dura-and-nerves-5d00527bd9fe4f3aba657f79e6231baa, a 3D volumetric model of the skull base after the brain has been removed [the outer dural layer was removed to show the relation of the PPsb and CN VI]). From an endonasal perspective, the ligament is posterior to CN VI (Fig. 2).

Laterally, the periosteal (outer) layer covers the PPsb and petrous apex to form the petroclival dural fold (PCDF). This dural fold is a key landmark because it forms the dural floor of the CS, where the abducens nerve transitions from the interdural to the proximal cavernous segment. This periosteal dural layer continues with the anterior wall of the CS and with the periosteum of the carotid canal.

Venous Relationships

The PPsb forms the floor of the posterior CS compartment, just behind the ICA (Fig. 3A). The lower limit of the CS is formed medially by the PPsb and laterally by the lingual process of the sphenoid bone (LPsb). Because the LPsb and PPsb are not in the same axial plane (Fig. 3C), the oblique line then defines the inferior limit of the CS.

The PPsb is located at the crossing of the petroclival venous confluence (PVC) and the CS (Fig. 3B). This space has an inverted trapezoid morphology with its minor base in a lower position. A line drawn from the PPsb to the posterior petroclinoidal dural fold marks the transition between the CS anteriorly and the PVC posteriorly. The basilar plexus drains into the medial aspect of the PVC and apex of the PPsb. The superior petrosal sinus (SPS) runs posteriorly to anteriorly and laterally to medially over the petrous ridge and lines the superior border of the trigeminal porus (Fig. 2). Then the SPS opens to the PVC posterolaterally to the PPsb. The inferior petrosal sinus (IPS) lies behind and lateral to the PPsb, with its upper part more medial than the lower part (see model 3, https://sketchfab.com/3d-models/transcranial-view-of-transclival-approach-78de008c7a8c4627a2d01c75b398d0d0, a 3D volumetric model of a cadaveric specimen with latex injection after brain removal that shows the relationship of the PPsb with the surrounding neurovascular structures).

Arterial Relationships

The apex of the PPsb marks the transition between the paraclival and parasellar ICA segments (Fig. 3D) and the transition from the extracavernous to the intracavernous course of the ICA (see model 3, https://sketchfab.com/3d-models/transcranial-view-of-transclival-approach-78de008c7a8c4627a2d01c75b398d0d0). In an axial section at the level of the apex of the PPsb, the ICA is anterior to this process (Fig. 3C and D). The PCF is positioned in relation to the posterolateral aspect of the paraclival ICA.

The relationships of the PPsb with the branches of the meningohypophyseal trunk are shown in Fig. 4A–D. In all our specimens, the PPsb was below the dorsal meningeal artery (DMA). The DMA divides into a medial and a lateral branch (Fig. 4B). The medial branch runs inferiorly and medially through the PVC and basilar plexus, along the posterior aspect of the clivus, to vascularize the surrounding dura mater (Fig. 4F). The lateral branch courses posteriorly and laterally, running just medial to the abducens nerve in the PVC. It then furthers divides into a medial branch, which runs with CN VI inside Dorello's canal and vascularizes the nerve, and a lateral branch, which supplies the dura mater of the petrous bone apex and the IPS[24,25] (Fig. 4F). During surgery, great care should be taken when coagulating and transecting these branches, given their close spatial relationship with the abducens nerve.

Neural Relationships

Abducens Nerve

CN VI exits the brainstem and follows a long path to reach the lateral rectus muscle into the orbit and is the only CN that runs inside 2 venous confluences, the CS and the PVC.[6,22] The CN VI course is divided into 4 segments: cisternal, interdural, intracavernous, and intraorbital[7,21] (Fig. 3D). The cisternal segment starts when the nerve exits the pontomedullary sulcus and crosses the prepontine cistern before piercing the inner clival dura. CN VI usually pierces the clival dura as a single trunk, but it may also do this as separated fascicules,[26] which was observed in 2 (20%) of our 10 specimens. CN VI then runs superiorly and laterally between both dural layers, traveling inside the PVC but outside the IPS (Fig. 3B). This interdural segment ends when the nerve bends above the PPsb and enters the posterior CS compartment (see model 2, https://sketchfab.com/3d-models/skull-base-dura-and-nerves-5d00527bd9fe4f3aba657f79e6231baa), changing from a vertical to an almost horizontal trajectory. The mean length of the interdural segment is 9 ± 1 mm. The cavernous segment turns laterally to enter the inferior CS compartment, which is lateral and inferior to the intracavernous horizontal ICA and continues into the lateral compartment of the CS to reach the superior orbital fissure (orbital segment). The PPsb marks the transition between the interdural and cavernous segments (Fig. 3C; model 3, https://sketchfab.com/3d-models/transcranial-view-of-transclival-approach-78de008c7a8c4627a2d01c75b398d0d0). At this point, the nerve is just covered by

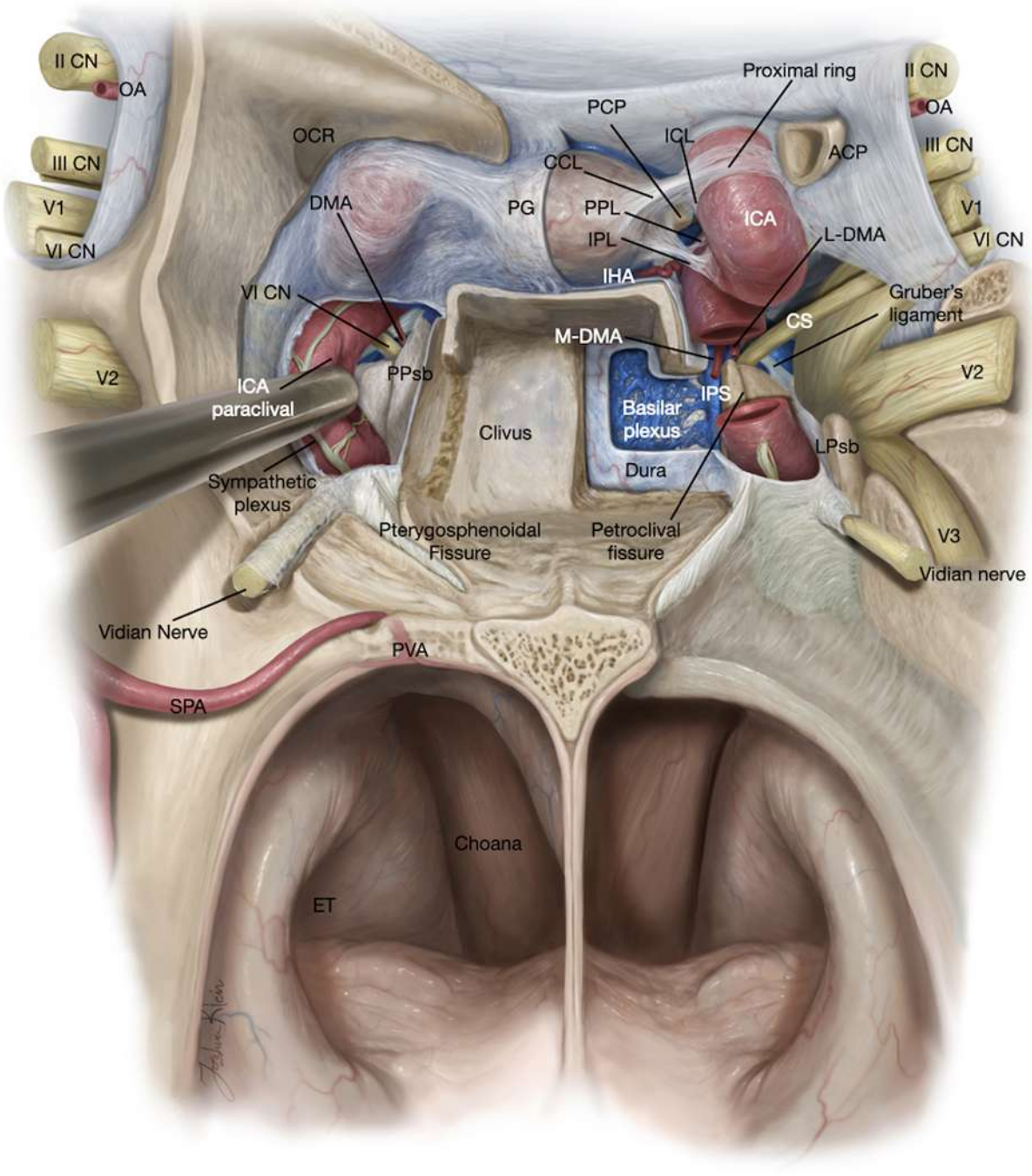

FIG. 2. Anatomical illustration of the petrosal process of the sphenoid bone (PPsb). Anterior view of the sphenoid sinus with different levels of dissection. On the right side, the floor of the sinus was drilled to simulate surgical exposure of the paraclival internal carotid artery (ICA). The retraction of the paraclival ICA allows visualization of the PPsb. On the right side, further dissection is shown, with the clivus drilled and the dura opened to show the basilar plexus. The paraclival ICA has been cut to show cranial nerve (CN) VI, Gruber's ligament, the inferior petrosal sinus (IPS), and the SPS after the drilling of the PPsb. Superiorly, the sella bone has been removed and the dura opened to show the parasellar ligaments. More laterally, the cavernous sinus (CS) has been dissected to show the relation of the CNs running inside it. ACP = anterior clinoid process; CCL = caroticoclinoid ligament; ET = eustachian tube; ICL = interclinoid ligament; IHA = inferior hypophyseal artery; IPL = inferior parasellar ligament; L-DMA = lateral branch of the dorsal meningeal artery; LPsb = lingual process of the sphenoid bone; M-DMA = medial branch of the dorsal meningeal artery; OA = ophthalmic artery; OCR = optic-carotid recess; PCP = posterior clinoid process; PG = pituitary gland; PPL = posterior parasellar ligament; PVA = palatovaginal artery; SPA = sphenopalatine artery; V1 = first branch of the trigeminal nerve; V2 = second branch of the trigeminal nerve; V3 = third branch of the trigeminal nerve. With permission from Juan C. Fernandez-Miranda and *The Neurosurgical Atlas* by Aaron A. Cohen-Gadol. Figure is available in color online only.

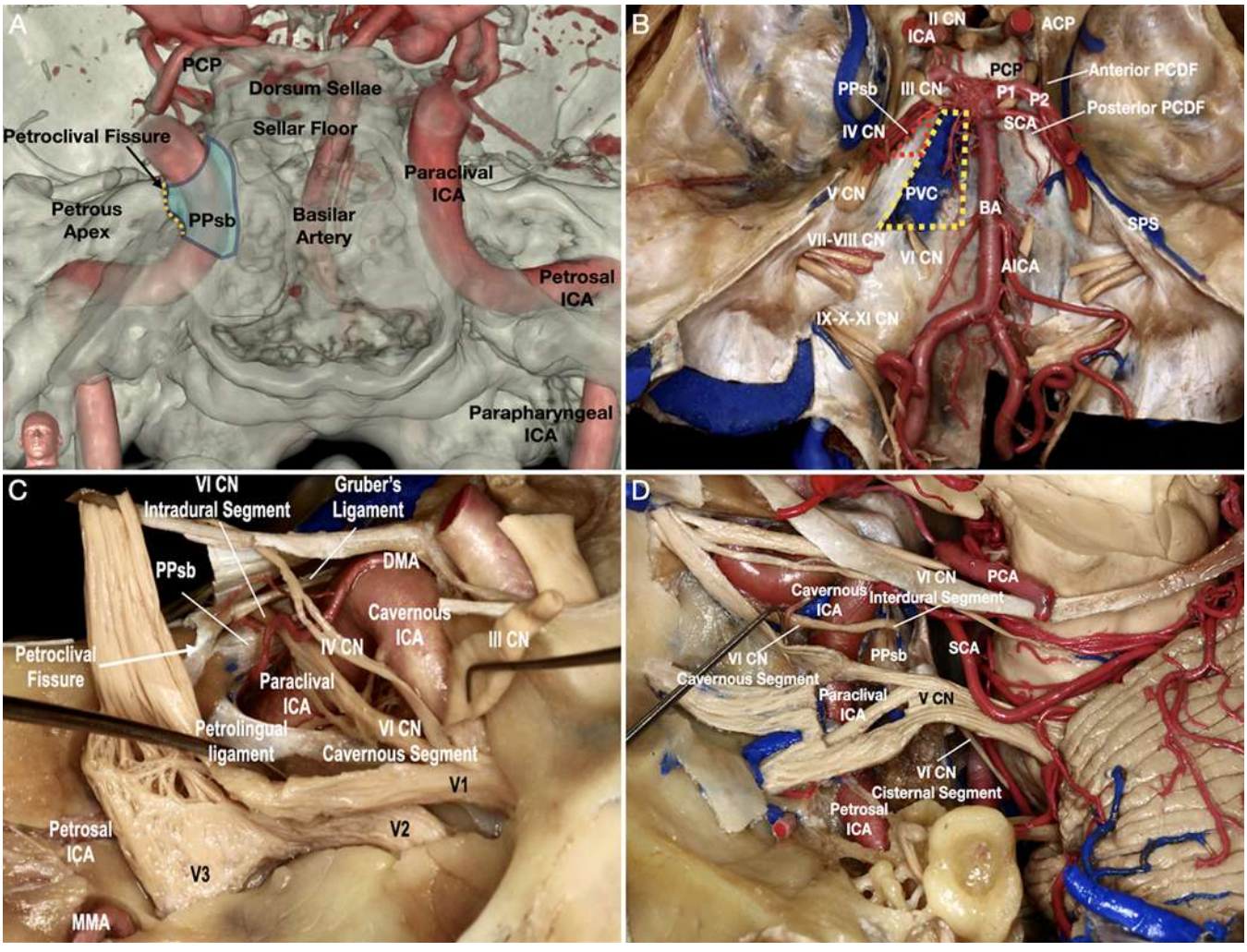

FIG. 3. Neurovascular relationships. **A:** Anteroposterior view of a skull base CT angiography reconstruction. The petrosal process of the sphenoid bone (PPsb) (*blue shading*) is posterior to the paraclival internal carotid artery (ICA) and demarks the transition between the extracavernous and intracavernous segments. The PCF (*yellow dotted line*) is lateral to the ICA. The 3D reconstruction was created from CT angiography using Surgical Theater software (Surgical Theater, LLC). **B:** The brain has been removed, preserving the cranial nerves (CNs) and vascular structures. The inner dural layer has been partially opened on the left side to show CN VI running inside the petroclival venous confluence (PVC) (*yellow dotted trapezoid*) but outside the IPS. The PPsb location is highlighted (*red dotted triangle*). **C:** Lateral view of the lateral wall of the right CS. The PPSb is shown posterior to the ICA and inferior to CN VI. The course of CN VI can be observed inside the CS. CN V is retracted inferiorly to show the PLL, which together with the PPsb forms the inferior limit of the CS. **D:** Overview of the course of CN VI and the carotid artery. The petrous bone has been drilled to show the prepontine cistern and the cisternal segment of CN VI, as well as the petrous segment of the ICA. The PPsb marks the transition between the interdural and cavernous segments of CN VI and the transition between the paraclival and the cavernous ICA. ACP = anterior clinoid process; AICA = anterior inferior cerebellar artery; BA = basilar artery; DMA = dorsal meningeal artery; MMA = middle meningeal artery; P1 = p1 segment of the posterior cerebral artery; P2 = p2 segment of the posterior cerebral artery; PCDF = petroclival dural fold; PCP = posterior clinoid process; SCA = superior cerebellar artery; SPS = superior petrosal sinus; V1 = first branch of the trigeminal nerve; V2 = second branch of the trigeminal nerve; V3 = third branch of the trigeminal nerve. With permission from Juan C. Fernandez-Miranda and *The Neurosurgical Atlas* by Aaron A. Cohen-Gadol. Figure is available in color online only.

arachnoid tissue. CN VI is inferomedial to the opening of the SPS into the PVC and medial to the trigeminal porus.

Trigeminal Nerve

The PPsb is medial to the trigeminal porus (Fig. 4H; also see model 3, https://sketchfab.com/3d-models/transcranial-view-of-transclival-approach-78de008c7a8c4627a2d01c75b398d0d0). Between them lies the PCF, which marks the transition from the sphenoid to the temporal bone. The medial limit of the porus corresponds to the lateral limit of the CS.

Technical Nuance

In an EEAtt, the PPsb can be identified through an extradural dissection of the sellar floor,[27,28] which guides to the lateral edge of the dorsum sellae (Fig. 5A; also see

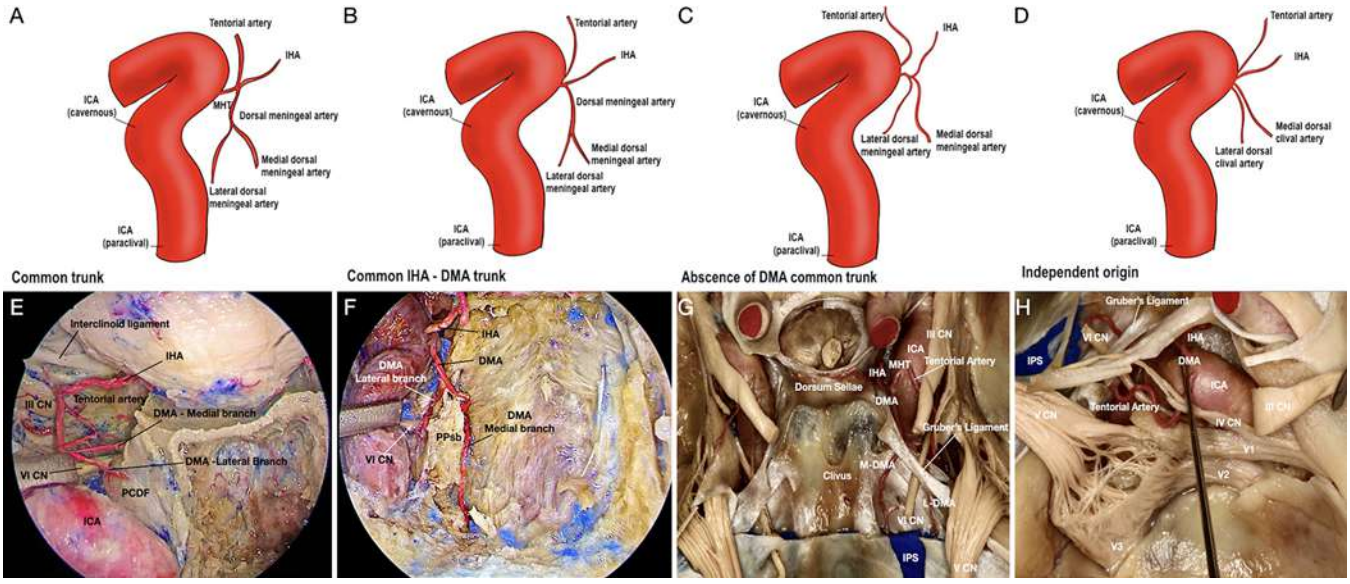

FIG. 4. Arterial relationships. A–D: Graphic drawings of the variants of the meningohypophyseal trunk (MHT). The MHT arises from the posterior wall of the posterior genu of the intracavernous internal carotid artery (ICA) and usually gives rise to 3 branches: the tentorial artery, the inferior hypophyseal artery (IHA), and the dorsal meningeal artery (DMA). **A:** In this study, 4 (40%) specimens had a common trunk, and in 6 (60%) specimens, the tentorial artery arose as a single branch. **B:** Of these specimens, 4 (40%) had a trunk giving rise to both the IHA and the DMA. **C:** In 1 (10%) case, there was a trifurcation with the absence of a DMA common trunk. **D:** In 1 (10%) specimen, the medial and lateral branches of the DMA and the IHA arose separately. **E:** Endoscopic view of the MHT branches. A common trunk pattern can be observed. The IHA runs to the posterior lobe of the pituitary gland. The tentorial branch runs upward to the roof of the CS. The DMA runs above the petrosal process of the sphenoid bone (PPsb) and divides into the medial and lateral branches. **F:** Divisions of the DMA. The medial branch supplies the clival dura, while the lateral branch runs laterally with cranial nerve (CN) VI. **G:** The lateral branch divides into a lateral branch, which heads to the petrous apex (PA), and a medial branch, which runs inside the PVC with CN VI. **H:** The PPsb is medial to CN V, which lies on the PA. IPS = inferior petrosal sinus; L-DMA = lateral branch of the DMA; M-DMA = medial branch of the DMA. With permission from Juan C. Fernandez-Miranda and *The Neurosurgical Atlas* by Aaron A. Cohen-Gadol. Figure is available in color online only.

model 4, https://sketchfab.com/3d-models/sphenoid-sinus-endoscopic-view-2-dfc832c17dae47f8a4c5a9e03a027a5d, a 3D volumetric model of the endoscopic surgical corridor showing the sphenoid sinus with exposure of the pituitary gland, ICA, and PPsb). This rim leads inferiorly to the PPsb and superiorly to the PCP. CN VI is hidden behind and above the PPsb. To expose this segment, the ICA has to be fully exposed and gently mobilized laterally to allow the base of the PPsb to be drilled out (Fig. 5B). After drilling of its base, the PPsb can be detached and removed with a blunt dissector. This procedure exposes the PCDF, which then can be opened to expose CN VI and the floor of the CS. CN VI runs a mean of 2 ± 0.5 mm lateral to the PCDF. At this point, the medial branch of the DMA can be identified running just medial to CN VI and the petrosphenoidal ligament behind CN VI, which serve as additional landmarks (Fig. 5C). Moreover, when the PPsb is removed, the IPS is exposed posteriorly (Fig. 5D and E). To identify the inferolateral limit of the CS, as well as the LPsb, additional bone removal is required in the anterior and lateral aspect of the paraclival ICA (Fig. 5F).

In a transcranial middle fossa approach, the PPsb is hidden inside the CS, and opening of the lateral wall is required to expose it. After performing a middle fossa approach using the Dolenc technique as described previously,[16] the lateral limit of the CS can be identified. Underneath CN V lies the petrolingual ligament (PLL), which is the posteroinferior attachment of the inner layer of the lateral wall of the CS.[29] The PPsb and PLL can be reached through the infratrochlear triangle (Fig. 6A), although exposing the PLL through this route is more difficult because of its more inferior location. The transition between the interdural and cavernous segments of CN VI can be identified above the PPsb. Drilling the PPsb enables the surgeon to retract the nerve inferiorly by a mean of 3 ± 0.7 mm to increase access to the posterior compartment of the CS[30] and upper PCF. From a posterolateral view through a transpetrosal approach or a combined transpetrosal approach,[18] the PPsb can be identified medially, after drilling of the petrous apex and opening of the clival dura, which forms the posterior wall of the PVC[31] and CS. Opening this dural layer also provides access to the interdural segment of CN VI (Fig. 6B).

Illustrative Clinical Cases

Case 1: EEAtt for Petroclival Chordoma

Presentation and Examination

A 14-year-old boy with a history of clival chordoma presented with seizure. He underwent a fronto-orbitozygomatic approach with partial resection of the tumor. Postoperative imaging showed residual tumor in the clivus, dorsum sella, posterior clinoid, and brainstem (Video 1).

VIDEO 1. Illustrative case 1 showing an EEAtt for the removal of

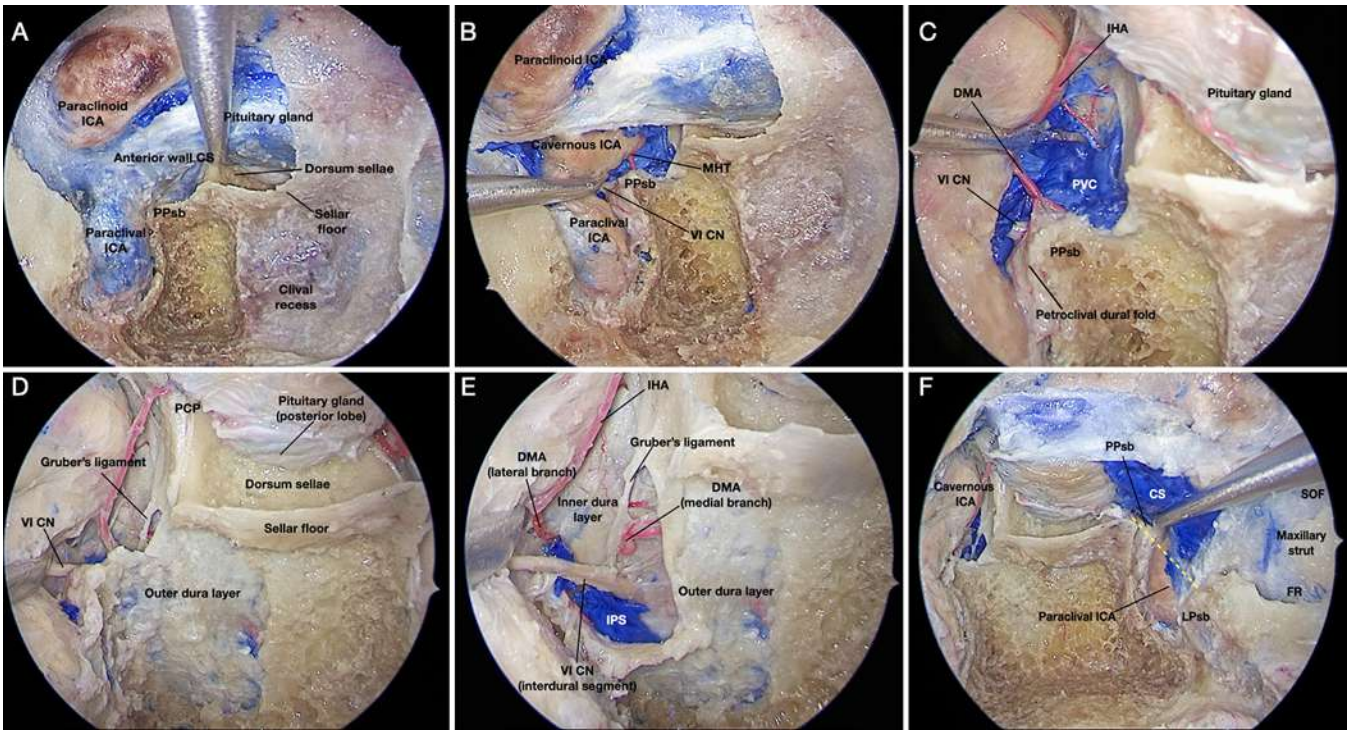

FIG. 5. Step-by-step identification and removal of the petrosal process of the sphenoid bone (PPsb) through an EEAtt. **A:** The bone of the sphenoid sinus on the right side has been partially removed, and the clival recess has been partially drilled on the right side. Following laterally the sellar floor in an extradural manner leads to the PPsb. **B:** The PCDF has been opened as well as the dura covering the right paraclival internal carotid artery (ICA), up to the proximal dural ring. **C:** Closer view showing the relationship of the PPsb with the surrounding neurovascular structures. Cranial nerve (CN) VI can be seen emerging through the petroclival venous confluence (PVC) and running lateral to the PPsb. The dorsal meningeal artery (DMA) relates to CN VI, and the medial and lateral division of this artery can be seen above the PPsb. **D:** The bone of the clivus has been drilled completely, preserving the petrosal process, and the blue silicone of the PVC has been removed. The outer dural layer is shown beneath the bone. Gruber's ligament runs posterior to the outer dural layer and CN VI. **E:** The PPsb has been removed and the outer dural layer has been opened, showing the interdural segment of CN VI. Gruber's ligament remains posterior to CN VI running from the petrous apex to the dorsum sellae. **F:** The inferior limit of the cavernous sinus (CS) is shown on the left side (*yellow dotted line*). The PPsb is the inferomedial limit, whereas the LPsb is the inferolateral limit of the CS. This line also marks the transition between the paraclival (extracavernous) and the parasellar (intracavernous) ICA. FR = foramen rotundum; IHA = inferior hypophyseal artery; IPS = inferior petrosal sinus; LPsb = lingual process of the sphenoid bone; MHT = meningohypophyseal trunk; PCP = posterior clinoid process; SOF = superior occipitofrontal fasciculus. With permission from Juan C. Fernandez-Miranda and *The Neurosurgical Atlas* by Aaron A. Cohen-Gadol. Figure is available in color online only.

a petroclival chordoma. With permission from Juan C. Fernandez-Miranda. Click here to view.

Operation and Postoperative Course

An EEAtt with extended clivectomy to expose the sellar region and the paraclival ICA was performed. Identification of the PPsb was crucial for recognizing CN VI and, therefore, to allow safe opening of the CS and wider clival removal (Video 1). The postoperative course was uneventful, and postoperative MRI showed gross-total resection of the tumor.

Case 2: EEAtt for Petroclival Chondrosarcoma

Presentation and Examination

A 74-year-old woman presented with double vision, especially when looking to the right, without any other associated symptoms. The physical examination revealed a mild right CN VI palsy with no other deficits. An MRI study revealed an extraaxial contrast-enhancing lesion in the PCF that extended caudally to the jugular foramen, with increased intensity in T2-weighted images and decreased intensity in T1-weighted images (Fig. 7A and B). A CT scan revealed osseous destruction in the right middle and lower clivus.

Operation and Postoperative Course

Surgery via an EEAtt to the petrous apex and jugular foramen was performed. After the sphenoid sinus was opened, the ICA lacerum segment was first identified, and then a middle and inferior clivectomy was performed. Osseous invasion of the tumor in the base of the PPsb and lower clivus was identified. The apex of the PPsb was removed and the PCDF opened, enabling visualization of CN VI (Fig. 7C, Video 2).

VIDEO 2. Illustrative case 2 showing an EEAtt for the removal of a petroclival chondrosarcoma. With permission from Juan C. Fernandez-Miranda. Click here to view.

Histological examination confirmed the diagnosis of chon-

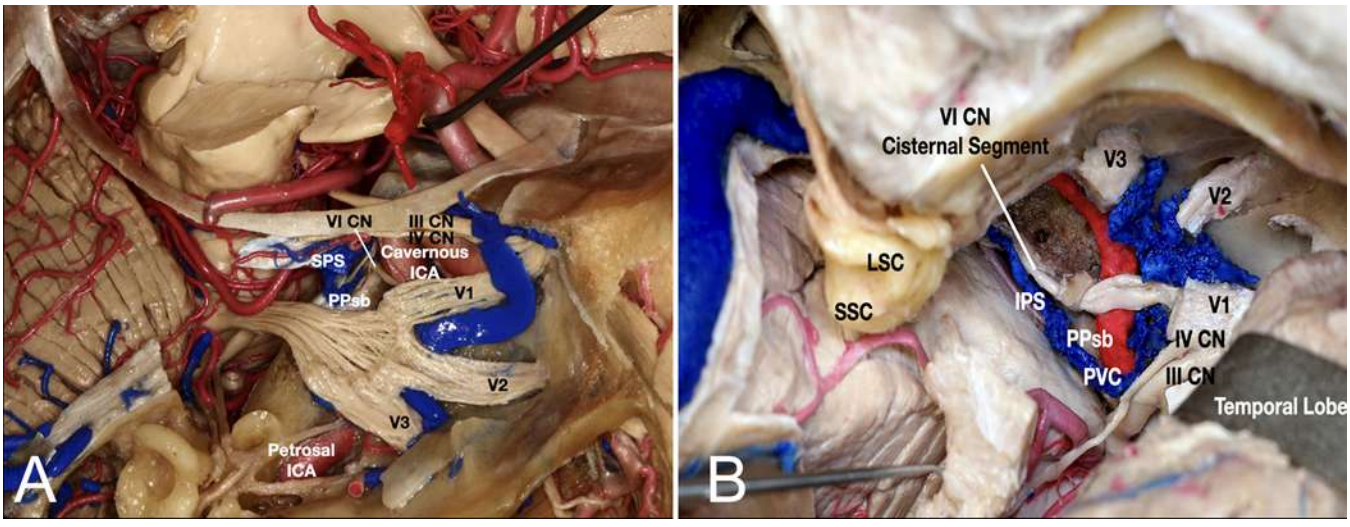

FIG. 6. Depiction of the lateral transcranial surgical view. **A:** Anterolateral approach. The lateral wall of the CS was opened, and V1 was retracted inferiorly. The petrosal process of the sphenoid bone (PPsb) is reached through Parkinson's triangle. The abducens nerve bends above the PPsb and turns laterally to the lateral compartment of the CS. **B:** Posterolateral approach. Combined middle fossa approach with partial removal of the labyrinth. The petrous apex was drilled, preserving the PPsb medially. The cisternal and interdural segments of the nerve can be seen. CN = cranial nerve; ICA = internal carotid artery; IPS = inferior petrosal sinus; LSC = lateral superior semicircular canal; PVC = petroclival venous confluence; SPS = superior petrosal sinus; SSC = superior semicircular canal; V1 = first branch of the trigeminal nerve; V2 = second branch of the trigeminal nerve; V3 = third branch of the trigeminal nerve. With permission from Juan C. Fernandez-Miranda and *The Neurosurgical Atlas* by Aaron A. Cohen-Gadol. Figure is available in color online only.

drosarcoma grade II. There were no postoperative complications, and the patient had complete resolution of her CN VI palsy after 2 days. Postoperative MRI showed a small remaining tumor in the jugular foramen; observation and Gamma Knife surgery in the case of growth were planned.

Case 3: EEAtt for Pituitary Macroadenoma

Presentation and Examination

A 31-year-old woman presented to the emergency department with progressive vision loss over 6 months, severe headaches, increased fatigue, and clinical stigmata of acromegaly with an elevated growth hormone level (8.9 ng/mL). A formal endocrinology workup revealed an elevated insulin-like growth factor 1 level (665 ng/mL); her other pituitary hormone levels were within normal limits. MRI of the pituitary gland with gadolinium contrast revealed an expanded (20 × 14 × 14 mm) sellar mass consistent with a pituitary adenoma with compression of the optic apparatus and invasion of the CS on the right side (Fig. 7D and E). MRI revealed significant disease burden in the superior and posterior compartments of the CS, with tumor extension behind the posterior genu of the carotid artery near the right CN VI. The tumor compressed the left CS without invading it.

Operation and Postoperative Course

The patient was taken to the operating room, and surgery via an EEAtt was performed. Resection of the medial wall of the CS on the right side and identification of the petrosal process were performed with gross-total resection of the mass. Exposure of the PPsb served as a necessary landmark for identifying the right CN VI and removing the lesion that was posterior to the carotid artery and predominantly in the inferior compartment in the CS (Fig. 7F). This operation resulted in normalization of the patient's postoperative growth hormone and insulin-like growth factor 1 levels 3 months after treatment without any pituitary dysfunction or CN palsy morbidity. Three-month follow-up MRI showed gross-total resection of the macroadenoma.

Discussion

The PPsb is the bony projection of the clival portion of the sphenoid bone that extends laterally behind the paraclival ICAs. The position of the PPsb laterally limits the middle clivus, which makes it a relevant structure during endoscopic transclival approaches, especially when a lateral extension is required (model 4, https://sketchfab.com/3d-models/sphenoid-sinus-endoscopic-view-2-dfc832c17dae47f8a4c5a9e03a027a5d). Due to the constant position and strategic location of the PPsb at the crossroads between the sagittal and coronal planes, it can be used as a landmark for several important structures, such as CN VI and the CS and ICA.

Abducens Nerve

Despite the use of intraoperative monitoring, localization of CN VI during surgery remains challenging.[32] For this reason, multiple landmarks for identifying it have been described, but none of them are accurate and easy to reproduce. Different types of injury of CN VI during surgery have been described,[7,8] such as injury during exposure or tumor removal, stretching of the nerve fibers during dissection, and damage to the nerve blood supply.

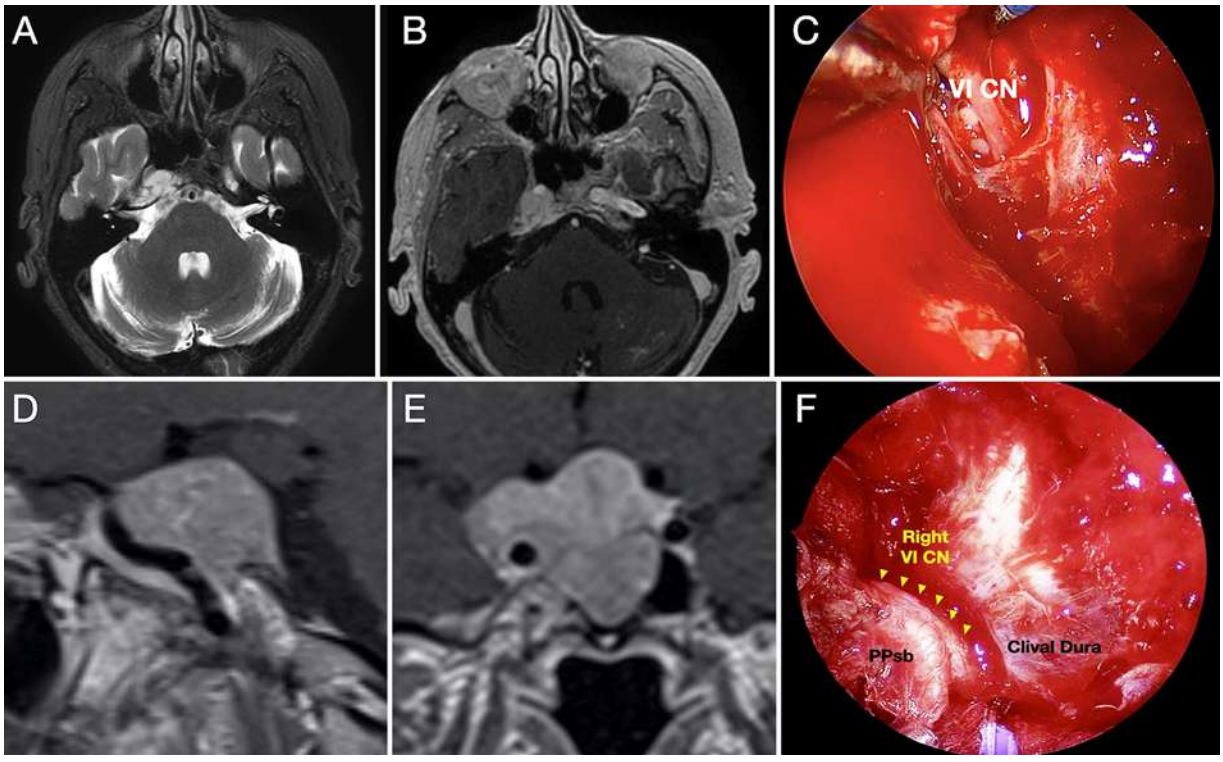

FIG. 7. Surgical application. A–C: Case 2. A 74-year-old woman presented with double vision caused by petroclival chondrosarcoma. **A:** Preoperative axial T2-FLAIR-weighted MR image showing a right petroclival lesion. **B:** Preoperative axial T1-weighted MR image with gadolinium contrast showing a contrast-enhancing lesion in the right petroclival fissure behind the posterior genu of the ICA. **C:** Intraoperative view of cranial nerve (CN) VI inside the PVC after drilling the petrosal process of the sphenoid bone (PPsb) and opening the outer dural layer and petroclival dural fold. D–F: Case 3. A 31-year-old woman presented with progressive vision loss and clinical stigmata of acromegaly with elevated growth hormone with CS invasion. **D:** Preoperative coronal T1-weighted MR image with gadolinium contrast showing a macroadenoma with invasion into the right CS. **E:** Preoperative sagittal T1-weighted MR image delineating significant invasion into the superior and posterior compartments of the CS with tumor extension behind the posterior genu of the ICA near the right CN VI. **F:** Intraoperative endoscopic view of CN VI coursing over the petrosal process, which is now covered with a sleeve of dura mater reflected over the bony process. With permission from Juan C. Fernandez-Miranda. Figure is available in color online only.

Destrieux et al.[31] described the PVC as the space through which CN VI courses from the prepontine cistern to the CS. In our study, Dorello's canal was inside the PVC in all our specimens. Therefore, Dorello's canal and the PVC are not equivalent. Dorello's canal goes just to the osteofibrous canal, but the PVC is a larger venous space within which CN VI courses.

Barges-Coll et al.[7] proposed the use of the lacerum segment of the ICA and sellar floor for identifying CN VI. As we have shown, the sellar floor is not on the same axial plane as CN VI when the nerve enters into the CS, but it is a mean of 3.5 ± 0.5 mm below it. Moreover, the lacerum segment of the ICA does not have a precise limit above the FL, which makes it difficult to recognize and thus unreliable as a landmark.[33]

Revuelta Barbero et al.[9] proposed using projection lines and angles from the eustachian tube as a landmark for CN VI during endoscopic endonasal surgery. Although this method is feasible, we consider it difficult to apply, because it requires a wide exposure and the estimation of lengths and angles.

Another landmark described is the inferolateral insertion of Gruber's ligament into the petrous apex.[10] While this feature can be an accurate surgical landmark, there are some limitations with its use. Although Gruber's ligament is present in most individuals, it can have some variations in shape or length or it can be hypoplastic.[23] Exposing the ligament from an endonasal approach can lead to CN VI injuries, because it is posterior to the nerve.

The PPsb is a constant structure that can be identified early during the EEAtt and thus before the exposure of CN VI. The interdural segment of CN VI is behind this process, and the transition to the cavernous segment is above and lateral to it (2 ± 0.5 mm). Indeed, as shown in the 3 surgical cases presented here, identification of the PPsb is an early and reliable landmark for CN VI and might decrease the risk of injury.

Cavernous Sinus

The CS has been divided into different compartments that can be identified by several key landmarks.[30,34] The PCF, the transition between the vertical and horizontal segments of the ICA and CN VI, has been proposed to be useful for localizing the inferior limit of the CS.[35] In the present study, we have shown that the PPsb, covered by

the PCDF, is the real inferior limit of the CS, and it can be used as a landmark in a reliable manner and at early steps in the surgery. Indeed, cutting the PCDF at the apex of the PPsb leads to venous bleeding from the posterior compartment of the CS.

Internal Carotid Artery

Subdivisions of the ICA that enable early identification of the artery during each step and through different surgical routes have been described.[35–38] These landmarks should be based on structures that have surgical relevance and can be recognized in an early, easy, and reliable manner. Alfieri and Jho[39] first described the terms "paraclival segment" and "parasellar segment" of the ICA, which have been widely used. The landmarks defined for identifying the transition between the paraclival and parasellar segments of the ICA, such as the medial petrous apex, PCF, and sellar floor, have several limitations. In our opinion, the PPsb could be used as a more precise landmark to differentiate these 2 segments from an endonasal view. Compared with the PCF, the PPsb can be identified in earlier steps of the surgery, because the PCF lies posterolateral to the PPsb and the paraclival ICA (Fig. 2). According to the literature[1] and our results, the sellar floor is not at the same level as the PCF or PPsb. Because the medial venous compartment of the CS sits below and lateral to the floor of the sella,[40] using the sellar floor as a landmark leads laterally to the intracavernous carotid, with a mean distance of 3.5 ± 0.5 mm from its entry point in the CS. Therefore, the PPsb can be used not only to define the distal limit of the paraclival ICA but also to mark, medially, the transition between the extracavernous and intracavernous courses of the ICA.

Study Limitations

The main limitation of this study is that it lacks clinical data pertaining to the abducens nerve and its function; therefore, we cannot demonstrate the efficacy of the proposed surgical landmarks for minimizing the risk of abducens nerve injury. Moreover, it is important to keep in mind that lesions invading the petroclival region and prepontine cistern will distort the normal anatomy, displacing the abducens nerve. The use of electrical stimulation is recommended when approaching these regions, before opening the dura and while resecting the tumor. Nevertheless, advanced knowledge of the normal anatomy, as described here, along with significant surgical experience, is crucial for predicting and understanding pathological variations in the location and the trajectory of the abducens nerve.[7]

Conclusions

The PPsb is a constant, useful, and reliable landmark that can be used to identify the abducens nerve during endoscopic endonasal surgery, potentially helping to minimize the risk of intraoperative nerve injury. Moreover, identification of the PPsb is significant for determining the placement of the lower and medial limits of the CS and also enables division of the course of the ICA into extracavernous or paraclival and intracavernous or parasellar segments.

Acknowledgments

We sincerely appreciate the support of the Stead Family Endowed Chair in the creation of this work. We also acknowledge Josh Klein for the outstanding anatomical illustration shown in Figure 2.

References

1. Kassam AB, Gardner P, Snyderman C, Mintz A, Carrau R. Expanded endonasal approach: fully endoscopic, completely transnasal approach to the middle third of the clivus, petrous bone, middle cranial fossa, and infratemporal fossa. *Neurosurg Focus*. 2005;19(1):E6.
2. Kassam A, Snyderman CH, Mintz A, Gardner P, Carrau RL. Expanded endonasal approach: the rostrocaudal axis. Part II. Posterior clinoids to the foramen magnum. *Neurosurg Focus*. 2005;19(1):E4.
3. Zwagerman NT, Zenonos G, Lieber S, et al. Endoscopic transnasal skull base surgery: pushing the boundaries. *J Neurooncol*. 2016;130(2):319-330.
4. Gardner PA, Tormenti MJ, Pant H, Fernandez-Miranda JC, Snyderman CH, Horowitz MB. Carotid artery injury during endoscopic endonasal skull base surgery: incidence and outcomes. *Neurosurgery*. 2013;73(2 suppl Operative):ons261-ons269.
5. Patel CR, Fernandez-Miranda JC, Wang WH, Wang EW. Skull base anatomy. *Otolaryngol Clin North Am*. 2016;49(1):9-20.
6. Iaconetta G, Fusco M, Cavallo LM, Cappabianca P, Samii M, Tschabitscher M. The abducens nerve: microanatomic and endoscopic study. *Neurosurgery*. 2007;61(3 suppl):7-14.
7. Barges-Coll J, Fernandez-Miranda JC, Prevedello DM, et al. Avoiding injury to the abducens nerve during expanded endonasal endoscopic surgery: anatomic and clinical case studies. *Neurosurgery*. 2010;67(1):144-154.
8. Jecko V, Sesay M, Liguoro D. Anatomical location of the abducens nerves (VI) in the ventral approach of clival tumors. *Surg Radiol Anat*. 2020;42(11):1371-1375.
9. Revuelta Barbero JM, Subramaniam S, Noiphithak R, et al. The Eustachian tube as a landmark for early identification of the abducens nerve during endonasal transclival approaches. *Oper Neurosurg (Hagerstown)*. 2019;16(6):743-749.
10. Tomio R, Toda M, Sutiono AB, Horiguchi T, Aiso S, Yoshida K. Grüber's ligament as a useful landmark for the abducens nerve in the transnasal approach. *J Neurosurg*. 2015;122(3):499-503.
11. Gray H. *Anatomy of the Human Body*. 20th ed. Lea & Febiger; 1918.
12. Kournoutas I, Vigo V, Chae R, et al. Acquisition of volumetric models of skull base anatomy using endoscopic endonasal approaches: 3D scanning of deep corridors via photogrammetry. *World Neurosurg*. 2019;129:372-377.
13. Rubio RR, Shehata J, Kournoutas I, et al. Construction of neuroanatomical volumetric models using 3-dimensional scanning techniques: technical note and applications. *World Neurosurg*. 2019;126:359-368.
14. Vigo V, Pastor-Escartín F, Doniz-Gonzalez A, et al. The Smith-Robinson approach to the subaxial cervical spine: a stepwise microsurgical technique using volumetric models from anatomic dissections. *Oper Neurosurg (Hagerstown)*. 2020;20(1):83-90.
15. Oyama K, Tahara S, Hirohata T, et al. Surgical anatomy for the endoscopic endonasal approach to the ventrolateral skull base. *Neurol Med Chir (Tokyo)*. 2017;57(10):534-541.
16. van Loveren HR, Keller JT, el-Kalliny M, Scodary DJ, Tew JM Jr. The Dolenc technique for cavernous sinus exploration (cadaveric prosection). *J Neurosurg*. 1991;74(5):837-844.
17. Hakuba A, Nishimura S, Tanaka K, Kishi H, Nakamura T. Clivus meningioma: six cases of total removal. *Neurol Med Chir (Tokyo)*. 1977;17(1 pt 1):63-77.

18. Janjua MB, Caruso JP, Greenfield JP, Souweidane MM, Schwartz TH. The combined transpetrosal approach: anatomic study and literature review. *J Clin Neurosci*. 2017;41:36-40.
19. Hamid O, El Fiky L, Hassan O, Kotb A, El Fiky S. Anatomic variations of the sphenoid sinus and their impact on transsphenoid pituitary surgery. *Skull Base*. 2008;18(1):9-15.
20. Rhoton AL Jr. The cavernous sinus, the cavernous venous plexus, and the carotid collar. *Neurosurgery*. 2002;51:S1-375-S1-410.
21. Joo W, Yoshioka F, Funaki T, Rhoton AL Jr. Microsurgical anatomy of the abducens nerve. *Clin Anat*. 2012;25(8):1030-1042.
22. Ziyal IM, Özgen T. The abducens nerve: microanatomic and endoscopic study. *Neurosurgery*. 2008;63(4):E820.
23. Icke C, Özer E, Arda N. Microanatomical characteristics of the petrosphenoidal ligament of Gruber. *Turk Neurosurg*. 2010;20(3):323-327.
24. Tekdemir I, Tüccar E, Çubuk HE, Ersoy M, Elhan A, Deda H. Branches of the intracavernous internal carotid artery and the blood supply of the intracavernous cranial nerves. *Ann Anat*. 1998;180(4):343-348.
25. Willinsky R, Lasjaunias P, Berenstein A. Intracavernous branches of the internal carotid artery (ICA). Comprehensive review of their variations. *Surg Radiol Anat*. 1987;9(3):201-215.
26. Coquet T, Lefranc M, Chenin L, Foulon P, Havet É, Peltier J. Unilateral duplicated abducens nerve coursing through both the sphenopetroclival venous gulf and cavernous sinus: a case report. *Surg Radiol Anat*. 2018;40(7):835-840.
27. Fernandez-Miranda JC, Gardner PA, Rastelli MM Jr, et al. Endoscopic endonasal transcavernous posterior clinoidectomy with interdural pituitary transposition. *J Neurosurg*. 2014;121(1):91-99.
28. Kassam AB, Prevedello DM, Thomas A, et al. Endoscopic endonasal pituitary transposition for a transdorsum sellae approach to the interpeduncular cistern. *Neurosurgery*. 2008;62(3 suppl 1):57-74.
29. Ziyal IM, Salas E, Wright DC, Sekhar LN. The petrolingual ligament: the anatomy and surgical exposure of the posterolateral landmark of the cavernous sinus. *Acta Neurochir (Wien)*. 1998;140(3):201-205.
30. Fernandez-Miranda JC, Zwagerman NT, Abhinav K, et al. Cavernous sinus compartments from the endoscopic endonasal approach: anatomical considerations and surgical relevance to adenoma surgery. *J Neurosurg*. 2018;129(2):430-441.
31. Destrieux C, Velut S, Kakou MK, Lefrancq T, Arbeille B, Santini JJ. A new concept in Dorello's canal microanatomy: the petroclival venous confluence. *J Neurosurg*. 1997;87(1):67-72.
32. López JR. Neurophysiologic intraoperative monitoring of the oculomotor, trochlear, and abducens nerves. *J Clin Neurophysiol*. 2011;28(6):543-550.
33. Bouthillier A, van Loveren HR, Keller JT. Segments of the internal carotid artery: a new classification. *Neurosurgery*. 1996;38(3):425-433.
34. Campero A, Campero AA, Martins C, Yasuda A, Rhoton AL Jr. Surgical anatomy of the dural walls of the cavernous sinus. *J Clin Neurosci*. 2010;17(6):746-750.
35. Labib MA, Prevedello DM, Carrau R, et al. A road map to the internal carotid artery in expanded endoscopic endonasal approaches to the ventral cranial base. *Neurosurgery*. 2014;10(suppl 3):448-471.
36. Fortes FSG, Pinheiro-Neto CD, Carrau RL, Brito RV, Prevedello DM, Sennes LU. Endonasal endoscopic exposure of the internal carotid artery: an anatomical study. *Laryngoscope*. 2012;122(2):445-451.
37. Herzallah IR, Casiano RR. Endoscopic endonasal study of the internal carotid artery course and variations. *Am J Rhinol*. 2007;21(3):262-270.
38. Kassam AB, Prevedello DM, Carrau RL, et al. The front door to Meckel's cave: an anteromedial corridor via expanded endoscopic endonasal approach—technical considerations and clinical series. *Oper Neurosurg (Hagerstown)*. 2009;64:ONS-71-ONS-83.
39. Alfieri A, Jho HD. Endoscopic endonasal cavernous sinus surgery: an anatomic study. *Neurosurgery*. 2001;48(4):827-837.
40. Yasuda A, Campero A, Martins C, Rhoton AL Jr, Ribas GC. The medial wall of the cavernous sinus: microsurgical anatomy. *Neurosurgery*. 2004;55(1):179-190.

Disclosures

The authors report no conflict of interest concerning the materials or methods used in this study or the findings specified in this paper.

Author Contributions

Conception and design: Fernandez-Miranda, Doniz-Gonzalez, Vigo, Mohyeldin. Acquisition of data: Fernandez-Miranda, Doniz-Gonzalez, Vigo, Nunez, Xu, Mohyeldin. Analysis and interpretation of data: Fernandez-Miranda, Doniz-Gonzalez, Vigo, Nunez, Xu, Mohyeldin. Drafting the article: Fernandez-Miranda, Doniz-Gonzalez, Vigo, Nunez, Xu, Mohyeldin. Critically revising the article: Fernandez-Miranda, Vigo, Nunez, Xu, Mohyeldin, Cohen-Gadol. Reviewed submitted version of manuscript: Fernandez-Miranda, Vigo, Doniz-Gonzalez, Xu, Cohen-Gadol. Approved the final version of the manuscript on behalf of all authors: Fernandez-Miranda. Statistical analysis: Fernandez-Miranda. Administrative/technical/material support: Fernandez-Miranda, Cohen-Gadol. Study supervision: Fernandez-Miranda, Cohen-Gadol.

Supplemental Information

Videos

Video 1. https://vimeo.com/659305664.
Video 2. https://vimeo.com/659308562.

Correspondence

Juan C. Fernandez-Miranda: Stanford Hospital, Stanford, CA. drjfm@stanford.edu.